PRE-CLINICAL RESEARCH

Cotransfection of Vascular Endothelial Growth Factor-A and Platelet-Derived Growth Factor-B Via Recombinant Adeno-Associated Virus Resolves Chronic Ischemic Malperfusion

Role of Vessel Maturation

Christian Kupatt, MD,* Rabea Hinkel, DVM,* Achim Pfosser, MD,* Chiraz El-Aouni, PhD,*
Alexander Wuchrer, MD,* Andrea Fritz, MD,* Franziska Globisch, MD,* Michael Thormann, DVM,*
Jan Horstkotte, MD,* Corinna Lebherz, MD,* Eckart Thein, DVM,† Andrea Banfi, PhD,‡
Peter Boekstegers, MD*

Munich, Germany; and Basel, Switzerland

Objectives   We set out to investigate the ability of cardiotropic adeno-associated viral vector (AAV2.9 = recombinant adeno-associated virus [rAAV]) to induce prolonged expression of vascular endothelial growth factor (VEGF)-A and platelet-derived growth factor (PDGF)-B in a rabbit hindlimb ischemia model and a pig model of hibernating myocardium.

Background   Gene therapy to induce angiogenesis and arteriogenesis has produced mixed results. However, long-acting viruses, such as rAAV, as well as combined induction of angiogenesis and vessel maturation might extend the therapeutic potential.

Methods   In rabbits, 0.5×10^{11} particles rAAV.VEGF-A with or without 1×10^{12} particles rAAV.PDGF-B were retroinfused at day 7 after femoral artery excision. At days 7 and 35, collateral counts and perfusion were determined, each value given as the day 35/day 7 ratio. Capillary-to-muscle fiber ratio was determined at day 35. In pigs, implantation of a reduction stent graft into the circumflex artery led to complete occlusion at day 28. At this time point, retroinfusion of rAAV.VEGF-A (1×10^{13} particles), rAAV.VEGF-A/PDGF-B (2×10^{12} and 4×10^{12} particles, respectively) or mock transfection was performed. Ejection fraction and left ventricular end-diastolic pressure were assessed at days 28 and 56.

Results   In rabbits, rAAV.VEGF-A strongly induced angiogenesis (capillary-to-muscle fiber ratio; 1.67 ± 0.09 vs. 1.32 ± 0.11 in rAAV.LacZ-treated limbs, $p < 0.05$), but not collateral growth ($125 \pm 7\%$ vs. $106 \pm 7\%$, $p = $ NS) or perfusion ($136 \pm 12\%$ vs. $107 \pm 9\%$, $p = $ NS). With VEGF-A/PDGF-B cotransfection, collateral growth increased to $146 \pm 9\%$, perfusion to $163 \pm 8\%$ of the respective day 7 value ($p < 0.05$). In the pig model, retroinfusion of rAAV.VEGF-A/PDGF-B increased regional myocardial blood flow reserve from $101 \pm 4\%$ (rAAV.Mock) to $129 \pm 8\%$ ($p < 0.05$), based on collateral growth (3.2 ± 0.3 in rAAV.Mock vs. 9.0 ± 0.4 in rAAV.VEGF-A/PDGF-B, $p < 0.05$), whereas rAAV.VEGF-A did not alter flow reserve ($112 \pm 7\%$) or collateral count (5.2 ± 0.7). rAAV.VEGF-A/PDGF-B improved ejection fraction ($55 \pm 5\%$ vs. $34 \pm 3\%$ in rAAV.Mock, $p < 0.05$) unlike rAAV.VEGF-A ($37 \pm 2\%$).

Conclusions   Retroinfusion of rAAV.VEGF-A alone induces angiogenesis, but fails to enhance collateralization and perfusion, unless PDGF-B is cotransfected. In addition to neovascularization, rAAV.VEGF-A/PDGF-B improves regional and global myocardial function in hibernating myocardium.   (J Am Coll Cardiol 2010;56:414–22) © 2010 by the American College of Cardiology Foundation

A growing number of patients with chronic ischemia of the heart or skeletal muscle caused by advanced atherosclerosis are not suitable for interventional or surgical treatment approaches. Therapeutic neovascularization has emerged as a novel treatment option from the basic insights into the biology of vessel growth. Growth factors such as vascular

endothelial growth factor (VEGF)-A have been demonstrated to increase small-vessel density and, although not always, perfusion (1). However, initial clinical trials with local delivery of angiogenic growth factors by adenoviral vectors yielded mixed results (2). Prominent among the many reasons are the efficacy of growth factor transfection, duration of expression, and the choice of agent(s) mediating vascular growth.

Therapeutic neovascularization appears to require the involvement of both microvascular and macrovascular processes. At the microcirculatory level, angiogenesis is defined as sprouting and growth of capillaries, which, however, regress after cessation of VEGF-A stimulation if pericytes have not been recruited (3). Therefore, stabilization of newly created capillary networks by mural cells (pericytes), known to be recruited by platelet-derived growth factor (PDGF)-B (4,5), is essential for therapeutic neovascularization. Insufficient recruitment of pericytes to newly formed capillaries and impaired maturation has been observed with uncontrolled VEGF-A overexpression (6–8), inducing at times leaky vessels (9) and even hemangioma growth (8,10). Consistent with these observations, VEGF-A has been identified as the major factor driving tumor angiogenesis (11), where vascularization is characterized by an irregular and often immature pattern (12). Of note, we recently found that PDGF-B coexpression can restore proper maturation of VEGF-A–induced microvessels, preventing hemangioma formation and increasing vessel functionality (A. Banfi et al., unpublished data, July 2009).

In addition to angiogenesis, arteriogenesis of collateral vessels, a distinct process of neovascularization, is necessary to reach therapeutic improvement of blood perfusion and muscle function. VEGF-A alone is not as efficient in inducing collateral growth (13,14) as other proarteriogenic (and proinflammatory) cytokines, such as monocyte chemoattractant protein-1, which act through monocyte recruitment (15).

Insufficient capillary maturation and paucity of arteriogenesis may partly explain the therapeutic failure of VEGF-A in clinical trials (16). Both processes require mural cell recruitment mediated by PDGF-B (4,6,17). To test the hypothesis that PDGF-B and mural cell recruitment can increase the therapeutic efficacy of VEGF-A, we conducted the present study using long-acting adeno-associated vectors encoding the cDNA of VEGF-A and PDGF-B to induce therapeutic neovascularization in large-animal models of limb and cardiac chronic ischemia.

Methods

All chemicals were purchased from Sigma (Taufkirchen, Germany), if not stated otherwise. Contrast agent Solutrast 370 was provided by Byk Gulden (Konstanz, Germany).
Virus production. The recombinant recombinant adeno-associated virus (rAAV). VEGF-A, rAAV.PDGF-B, and rAAV.LacZ vectors were produced using a triple transfection method, 1 plasmid encoding for the transgene (*VEGF-A*, *PDGF-B*, or *LacZ*) under control of a cytomegaly virus promoter flanked by the *cis*-acting AAV2 internal terminal repeats, a second plasmid providing AAV2 rep, and AAV9 cap in trans (18), whereas a third plasmid supplemented adenoviral helper function. Transfection was performed in 293 cells using polyethylenimine. Cells were harvested 48 h later and vectors purified with cesium gradients as described previously (19). Viral titers were determined using real-time polymerase chain reaction against the polyA tail of the vector bGH. Forward primer sequence was 5′-tctagttgccagccatctgttgt-3′ reverse primer sequence was 5′-tggggagtggcaccttcca-3′. As mock vector, we packaged the AAV without any coding sequence (rAAV.Mock) for transfection in the heart. This avoided potential functional interference due to an overexpressed reporter protein. Trans and helper plasmids were kindly provided by James M. Wilson, University of Pennsylvania.
Gene transfer detection. Real-time polymerase chain reaction was used for virus detection in transfected rabbit tissue. Primer sequences for VEGF-A were forward 5′TTTTACGCTATGTGGATACGC and reverse 5′GAGACAGCAACCAGGATTT; primer sequences for PDGF-B were forward 5′CCTCATAGACCGCACCAA and reverse 5′CGCACAATCTCGATCTTTCT. Real-time polymerase chain reaction was performed using SYBR green (Bio-Rad, Munich, Germany) for 40 cycles (30 s at 95°C, 30 s at 58°C, 30 s at 72°C) in an iQ-Cycler (Bio-Rad). Moreover, in the rabbit and pig model, VEGF-A and PDGF-B were detected by immunoblotting (Santa Cruz, Heidelberg, Germany) (20).
Animal protocols. All animal experiments were approved by the Bavarian Animal Care and Use Committee (AZ 211-2531-2531-82/02 and AZ 55.2-1-54-2531-67/07) and conformed to the Guide for the Care and Use of Laboratory Animals published by the U.S. National Institutes of Health (NIH publication no. 85-23, revised 1996, Approved Institution #A5637-01). All animal experiments were conducted at the Walter-Brendel Centre of Experimental Medicine.
Rabbit protocol. At day 0, New Zealand white rabbits (3.5 ± 0.4 kg, 6 per group for rAAV.LacZ and 5 each for rAAV.VEGF-A and rAAV.VEGF-A/PDGF-B) were anesthetized and subjected to excision of the complete right femoral artery (Online Fig. 1A) (21). At days 7 and 35, an angiography was performed after local infusion of adenosine (500 μg per animal) using automated contrast agent injection (1 ml/s, 4 ml total). Twenty-five angiographic frames per second were acquired and stored for later analysis (Ziehm, Nürnberg, Germany).

Abbreviations and Acronyms

LV = left ventricular

PDGF = platelet-derived growth factor

rAAV = recombinant adeno-associated virus

rAAV.Mock = recombinant adeno-associated virus without any coding sequence

VEGF = vascular endothelial growth factor

At day 7, the tibial anterior vein was surgically prepared and a polyethylene catheter was inserted. A ligature was placed around the femoral vein, gently closed, and fluoroscopic control of occlusion of venous outflow was performed (Online Fig. 1A). Thereafter, retroinfusion of 5 ml of phosphate-buffered saline containing 0.5×10^{11} particles of rAAV.LacZ or rAAV.VEGF-A with or without 1×10^{12} particles rAAV.PDGF-B was performed over 30 min at 80-mm Hg perfusion pressure.

Capillary density. Tissue samples from calf muscles (gastrocnemius, tibialis anterior, fibularis) were obtained for quantification of capillary density. Tissue was fixed in formaldehyde and embedded in paraffin. Capillaries stained by CD31 antibody SC1506 (Santa Cruz) and myofibers were counted in a blinded fashion in 5 microscopic fields (40× magnification) per muscle. NG-2 antibody (Chemicon, Hofheim, Germany) was used for pericyte detection.

Collateral growth, perfusion. Collaterals were assessed in a blinded fashion by counting the number of vessels in the femoral region intersecting an overlaying grid, as described previously (22). For assessment of perfusion, fluorescent microspheres were injected by a catheter into the left ventricle over 30 s. Arterial reference blood samples were drawn at a fixed rate. At the end of the experiment, samples were taken from thigh and calf muscles to assess blood flow in the upper and lower region of the ischemic hind limb and the nonischemic contralateral limb. After lysis, microsphere fluorescence was quantified in a Tecan Safire microplate reader, using the appropriate detection wavelength for each fluorescent microsphere type according to manufacturer's instructions.

Pig experiments. German farm pigs were anesthetized and instrumented as previously described (20). Briefly, ischemia was induced by placing a reduction stent (2.5×13 mm, Jomed, Munich, Germany) (23) into the proximal ramus circumflexus, inducing 75% stenosis that progressed to total occlusion at day 28 (Online Fig. 1B). A marker of gradual stent occlusion and an inclusion criterion was an area of infarcted myocardium <6% of the total left ventricular (LV) area at d56 (tetrazolium red staining). Infarct size was $3.1 \pm 1.1\%$ for rAAV.Mock, $2.4 \pm 0.8\%$ for rAAV.VEGF-A, and $2.1 \pm 0.4\%$ in the rAAV.VEGF-A/PDGF-B group. Of 27 animals entering the study after stent placement, 8 died due to sudden cardiac death during the first 28 days, whereas no animal died between days 28 and 56. Two animals were excluded because of myocardial infarction >6% of the LV mass. The remaining 17 animals were treated by mock transfection (6×10^{12} rAAV containing no transgene, n = 7), rAAV.VEGF-A transfection (1×10^{13} particles, n = 4), or rAAV.VEGF-A/PDGF-B transfection (2×10^{12} and 4×10^{12} particles, respectively, n = 6) via continuous pressure-regulated retroinfusion into the lateral vein, as described previously (20).

At day 56, subendocardial segment shortening was performed after placing sonomicrometry crystal pairs into the ischemic (circumflex artery perfused area) region and nor-malized to measurements in the control region (left anterior descending artery perfused area). Global myocardial function was assessed by means of a pressure tip catheter placed in the left ventricle (for LV end-diastolic and systolic pressures, dP/dt$_{max}$, dP/dt$_{min}$), whereas LV angiography was performed in anteroposterior position for the analysis of ejection fraction (yielding slightly smaller control values than a right anterior oblique view). Although one animal of the treatment group died during SES assessment, it provided all other data.

For assessment of regional myocardial blood flow, fluorescent microspheres (Molecular Probes, 5×10^6) were injected into the left atrium at each time point (day 28, day 56) at rest and during rapid pacing (150 beats/min), and appropriate reference blood samples were drawn. Systematic sampling of LV myocardium (23) revealed perfusion levels at baseline and rapid atrial pacing (140 beats/min, flow reserve) in the ischemic and nonischemic areas. Postmortem angiograms were obtained for visualization of collateral formation. Tissue from nonischemic and ischemic LV myocardium was used for determining the capillary-to-muscle fiber ratio (see previous text).

Statistical methods. The results are given as mean ± SEM. Statistical analysis of the results between >2 experimental groups was performed with 1-way analysis of variance, where appropriate, whereas 2-way analysis of variance was applied in all figures that compared >2 groups in >1 condition. Whenever a significant effect was obtained with analysis of variance, we performed multiple comparison tests between the groups using the Student-Newman-Keul procedure. Two experimental groups were compared using Student *t* test. All procedures were performed using SPSS version 17.0.2 (SSPS, Inc., Chicago, Illinois). Differences between groups were considered significant at p < 0.05.

Results

In the rabbit model of chronic hindlimb ischemia, rAAV delivery yielded a robust transduction of muscle tissue, as detected by LacZ reporter gene expression 4 weeks later (Online Fig. 2A). Transfection occurred throughout the treated hindlimb (i.e., in both the calf and thigh muscles). Approximately one-fifth of the hindlimb production rate was obtained in terms of polymerase chain reaction for the liver and <1/20 for the spleen and the kidneys (data not shown). Consistently, increased expression of VEGF-A and PDGF-B transcripts was detected in the ischemic hindlimb tissue 35 days after treatment with the therapeutic AAV compared with rAAV.Mock vector (Online Figs. 2B and 2C). Although no elevation of plasma levels of VEGF-A was detected by enzyme-linked immunosorbent assay, PDGF-B was found elevated at day 35 (from 1.2 ± 0.1 ng/ml to 2.1 ± 0.1 ng/ml, data not shown).

To assess the effects of PDGF-B coexpression on VEGF-induced angiogenesis, 0.5×10^{11} rAAV.VEGF-A particles
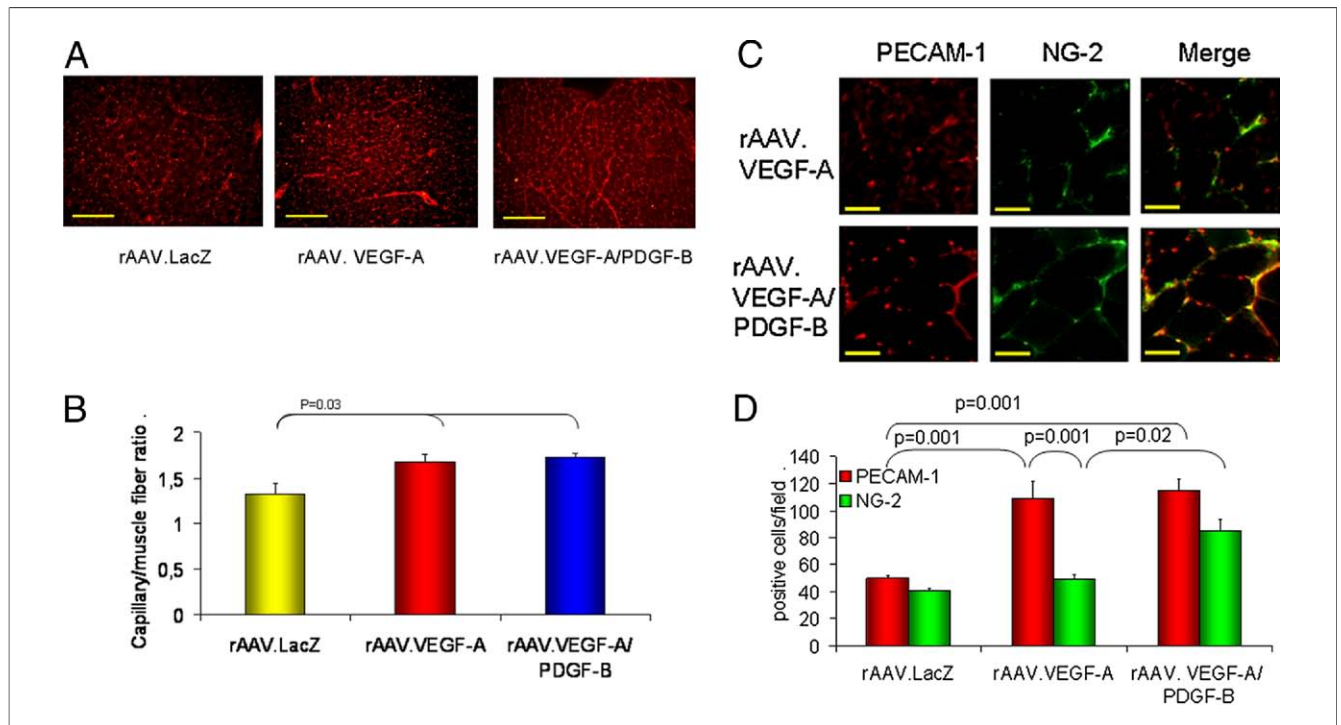
Figure 1 **VEGF-A/PDGF-B Transfection Induces Angiogenesis and Microvessel Maturation in Rabbit Hindlimbs**

Examples **(A)** and quantification **(B)** of PECAM-1 staining for capillary detection reveals an increased capillary/muscle fiber ratio in both vascular endothelial growth factor (VEGF)-A and VEGF-A/platelet-derived growth factor (PDGF)-B transfected animals (**yellow bar** = 200 μm). **(C)** As depicted in examples, coverage of PECAM-1–positive vascular structures with pericytes (detected by NG-2 antibody) was increased after combined VEGF-A/PDGF-B treatment compared with LacZ-transfected hindlimbs (**yellow bar** = 50 μm). **(D)** Quantitative analysis confirmed that capillary density and pericyte coverage increased after recombinant adeno-associated virus (rAAV).VEGF-A/PDGF-B transfection.

were retroinfused into the ischemic hindlimbs with or without 1×10^{12} rAAV.PDGF-B particles. VEGF-A alone caused an increase in capillary-to-muscle fiber ratio from 1.32 ± 0.11 to 1.67 ± 0.09 (p < 0.05) compared with control LacZ virus (Figs. 1A and 1B), although the induced network appeared slightly irregular (Fig. 1A). Moreover, a large proportion of vessels induced by VEGF alone were immature, as indicated by the lack of coverage with NG-2–positive pericytes (Figs. 1C and 1D). Codelivery of the rAAV.VEGF-A/PDGF-B combination did not further increase the capillary-to-muscle fiber ratio (1.73 ± 0.04) in the calf musculature compared with VEGF-A alone (Figs. 1A and 1B), but significantly increased pericyte coverage of the induced vessels (p = 0.02) (Figs. 1C and 1D).

The functional effects of rAAV delivery were determined by quantifying collateral artery growth and vascular perfusion in ischemic hindlimbs at the time of treatment (day 7) and after 4 weeks (day 35). Angiographic analysis (representative examples are shown in Fig. 2A) demonstrated that rAAV.VEGF-A alone did not induced growth of collateral arteries compared with rAAV.LacZ (125 ± 8% vs. 106 ± 7% for rAAV.LacZ, each compared with the respective level at day 7; p = NS), whereas the collateral growth was significantly increased by codelivery of PDGF-B (146 ± 8%, p < 0.05 vs. rAAV.LacZ) (Fig. 2B). Consistent with the lack of collateral growth, perfusion was not enhanced by

rAAV.VEGF-A alone (128 ± 11% vs. 110 ± 6% for rAAV.LacZ, each compared with the respective level at day 7, p = NS), but it was greatly improved when rAAV.PDGF-B was coapplied (189 ± 14%, p < 0.05 vs. both, rAAV.VEGF-A and rAAV.LacZ) (Fig. 2C). Thus, only the combination of VEGF-A and PDGF-B induced both microvascular and macrovascular growth (i.e., generation of pericyte-covered capillaries and an increase in collaterals, with a subsequent improvement of perfusion).

To prove the therapeutic relevance of the VEGF-A/PDGF-B combination also in cardiac ischemia, we next investigated its impact on a preclinical model of chronic myocardial hibernation in pigs. A reduction stent was used to gradually induce chronic total occlusion of the target coronary artery and hibernating myocardium at 4 weeks. At this time point, either an empty vector control (rAAV.Mock), rAAV.VEGF-A alone, or the rAAV.VEGF-A/PDGF-B combination was retroinfused via the lateral vein. Western blot analysis confirmed sustained overexpression of VEGF-A and PDGF-B protein 4 weeks after treatment with rAAV.VEGF-A/PDGF-B compared with rAAV.Mock (Online Figs. 3A and 3B). At day 56, the combined treatment caused a significant increase in both capillary density (detected by PECAM-1 staining) and pericyte coverage (detected by NG-2 staining) in the ischemic region (Fig. 3). Of note, VEGF-A alone, al-
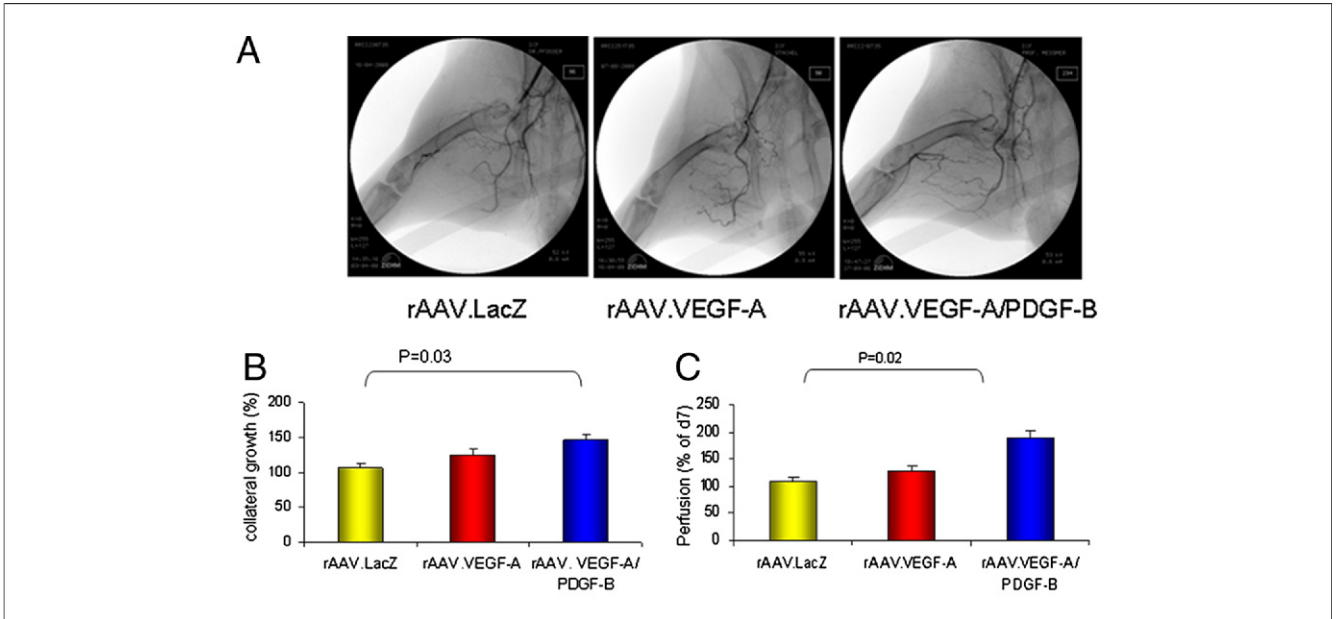
Figure 2   VEGF-A/PDGF-B Escalates Collateral Growth and Perfusion in Rabbit Hindlimbs

Examples **(A)** and quantification **(B)** of collateral count (see Methods section) reveals that VEGF-A increases collateral growth only if combined with PDGF-B.
(C) Fluorescent microsphere analysis revealed an increase in blood flow only after transfection of both VEGF-A/PDGF-B (5 per group). Abbreviations as in Figure 1.

though inducing a 2.1-fold increase in capillary density, failed to increase pericyte recruitment (Fig. 3B).

Similarly, the number of angiographically visible collaterals was greatly increased in the VEGF-A/PDGF-B–treated group (9.0 ± 0.4) compared with the rAAV.Mock group (2.7 ± 0.5, p = 0.001) (Figs. 4A and 4B), whereas VEGF-A transduction caused only a modest, although significant, increase (Fig. 4B). The Rentrop score (24) of

functioning collaterals (0 = no filling, 1 = side branch filling, 2 = partial main vessel filling, 3 = complete main vessel filling) also indicated a pronounced effect of the VEGF-A/PDGF-B combination (2.4 ± 0.2 vs. 1.1 ± 0.2, p = 0.02), whereas VEGF-A alone exerted no effect (Fig. 4C). Consistent with the assessment of collateral development, quantification of blood flow by fluorescent microspheres indicated an attenuation of perfusion in the
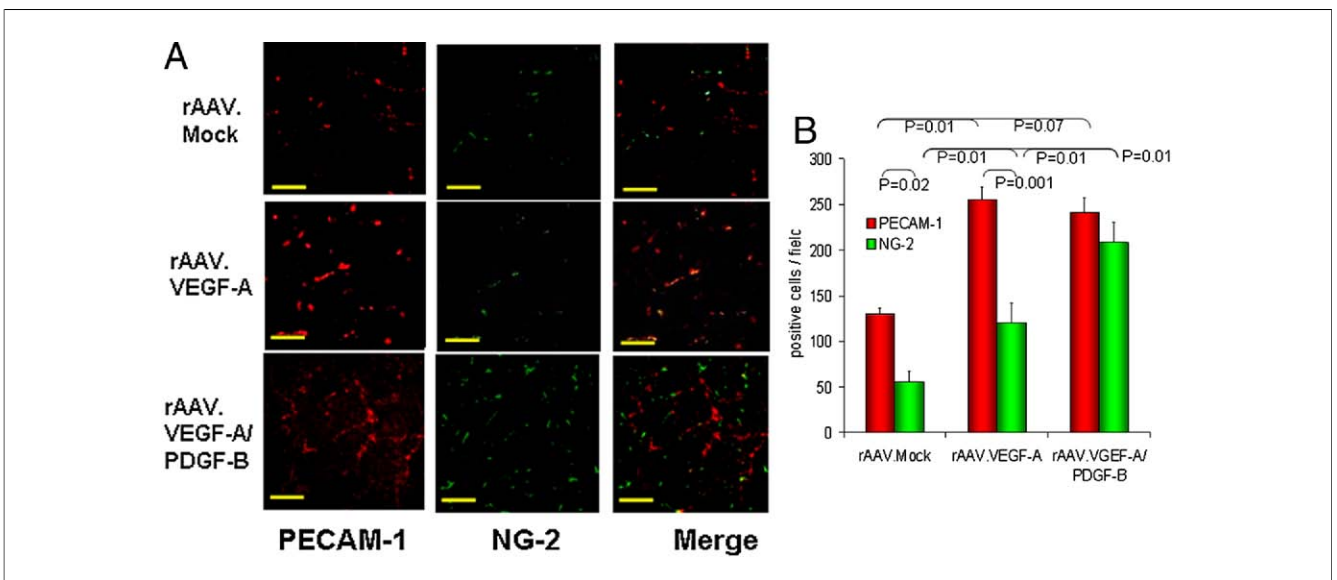
Figure 3   VEGF-A/PDGF-B Induces Angiogenesis and Vessel Maturation in Hibernating Myocardium (Pigs)

Examples **(A)** and quantification **(B)** of PECAM-1 (endothelial cells) and NG-2 (pericyte) expression in ischemic myocardium after transfection with
rAAV.Mock, rAAV.VEGF-A (1×10^{13} particles), or rAAV.VEGF-A/PDGF-B ($2 \times 10^{12}/4 \times 10^{12}$ particles) (**yellow bar** = 50 μm). Abbreviations as in Figure 1.
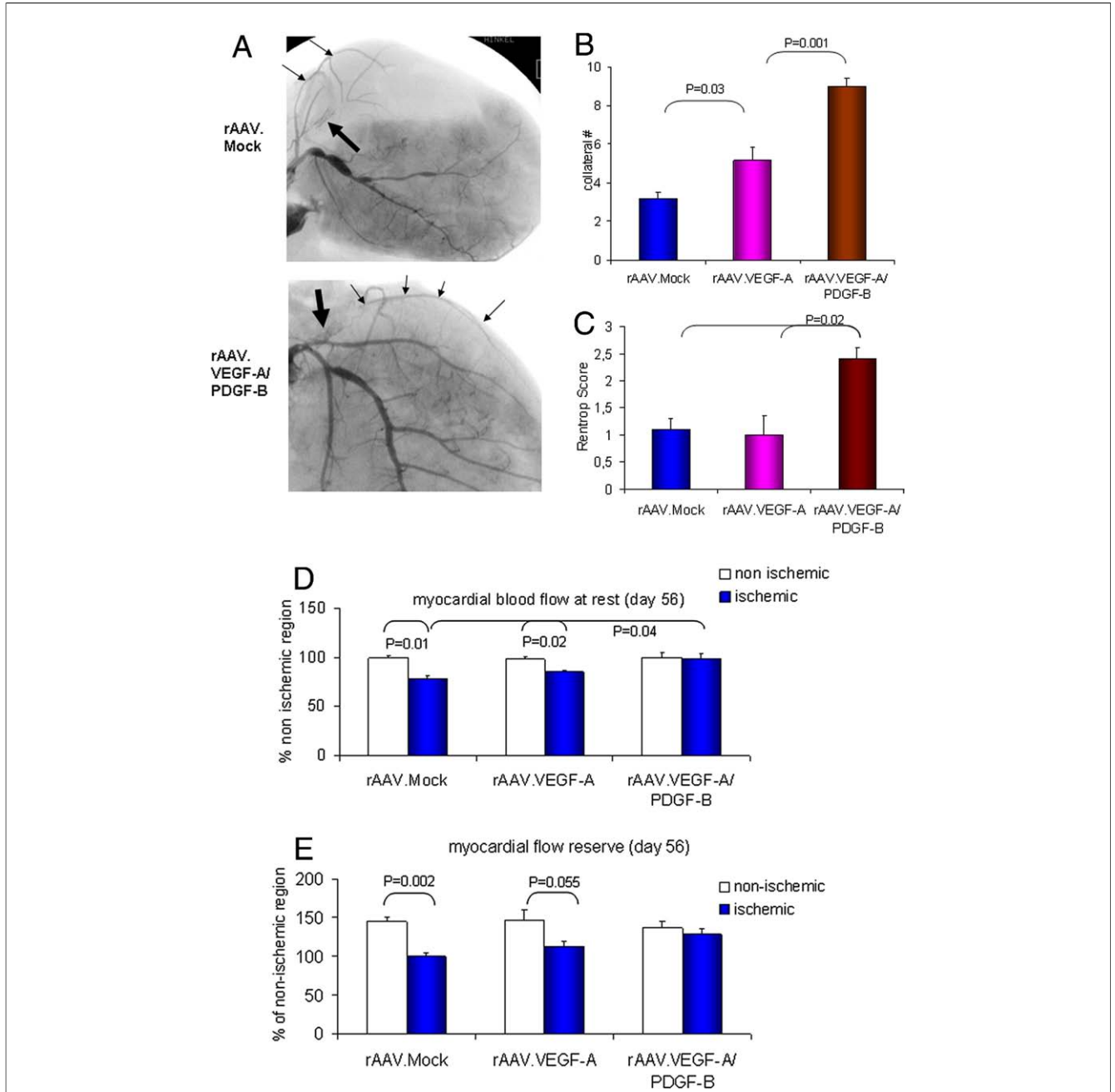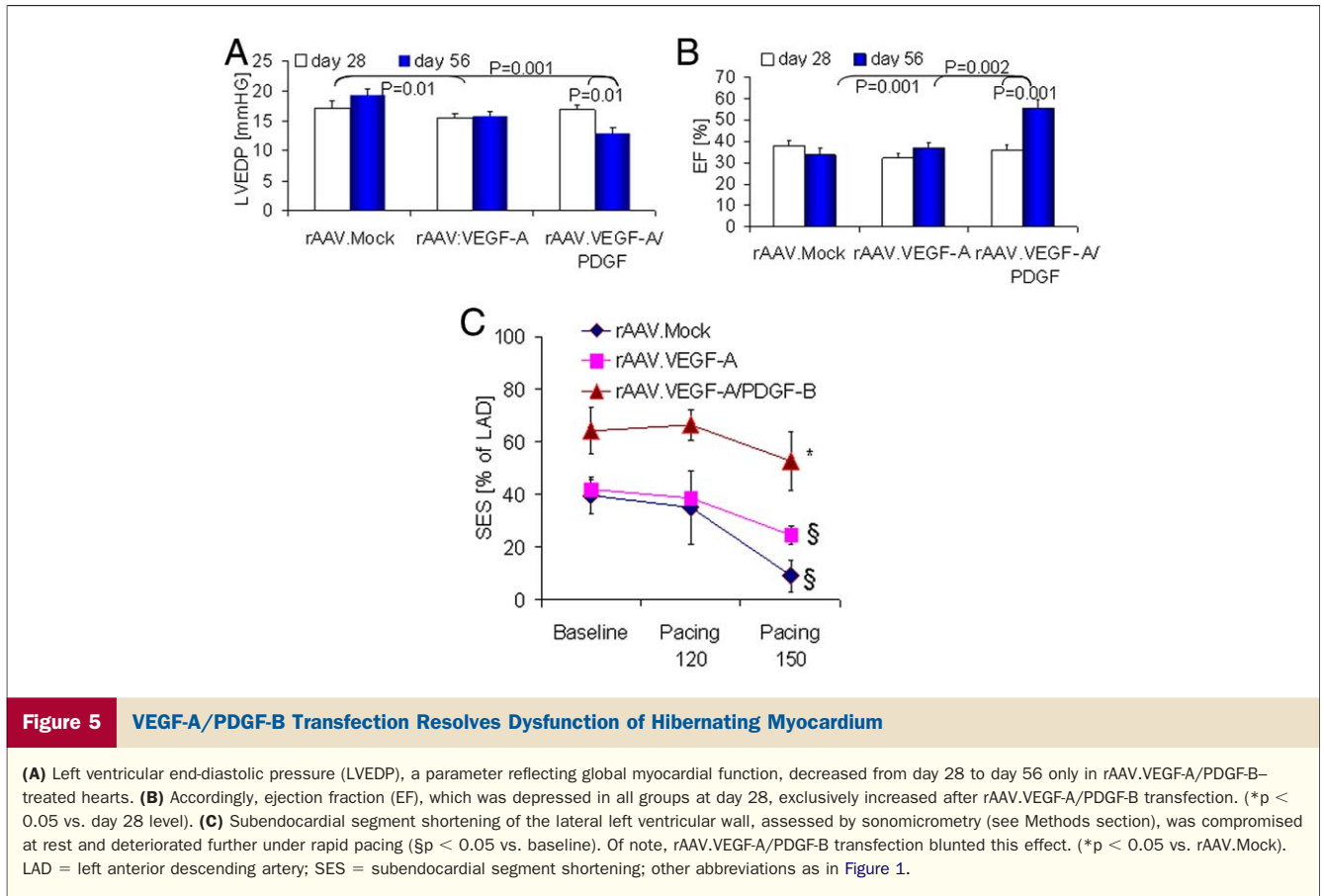
Figure 4   Collateralization and Blood Flow Increase After VEGF-A/PDGF-B Transfection of Pigs

Examples **(A)** and quantification **(B)** of angiographically visible collaterals in Mock- or VEGF-A/PDGF-B transfected pigs (**arrows** indicate collateral formation, #p < 0.05 vs. Mock). **(C)** Rentrop score indicates a gain of functional collateralization only after VEGF-A/PDGF-B transfection. Microsphere analysis revealed a decreased perfusion of the ischemic myocardium at rest **(D)** and under rapid pacing (150/min) **(E)** beats, which was corrected by transfection with rAAV.VEGF-A/PDGF-B, but not with VEGF-A alone. Abbreviations as in Figure 1.

territory of the circumflex artery in rAAV.Mock and VEGF-A virus-treated hearts, which was completely alleviated by treatment with rAAV.VEGF-A/PDGF-B (77 ± 2%, 85 ± 2% vs. 97 ± 5% of resting nonischemic tissue, respectively, p = 0.04) (Fig. 4D). To quantify the perfusion reserve of myocardial tissue, blood flow was also measured during atrial pacing at 150 beats/min (Fig. 4E). Perfusion readily increased in nonischemic tissue (144 ± 6% of resting nonischemic myocardium, p = 0.002). In contrast, ischemic tissue was unable to increase perfusion beyond resting values in the rAAV.Mock group (101 ± 4%), revealing a significantly impaired coronary flow reserve (p = 0.002). Hearts treated with rAAV-VEGF-A tended to improve coronary flow reserve (112 ± 7% in the ischemic area vs. 147 ± 12%

Figure 5 **VEGF-A/PDGF-B Transfection Resolves Dysfunction of Hibernating Myocardium**

(A) Left ventricular end-diastolic pressure (LVEDP), a parameter reflecting global myocardial function, decreased from day 28 to day 56 only in rAAV.VEGF-A/PDGF-B–treated hearts. **(B)** Accordingly, ejection fraction (EF), which was depressed in all groups at day 28, exclusively increased after rAAV.VEGF-A/PDGF-B transfection. (*p < 0.05 vs. day 28 level). **(C)** Subendocardial segment shortening of the lateral left ventricular wall, assessed by sonomicrometry (see Methods section), was compromised at rest and deteriorated further under rapid pacing (§p < 0.05 vs. baseline). Of note, rAAV.VEGF-A/PDGF-B transfection blunted this effect. (*p < 0.05 vs. rAAV.Mock). LAD = left anterior descending artery; SES = subendocardial segment shortening; other abbreviations as in Figure 1.

in nonischemic tissue, p = 0.055). Of note, a gain in coronary flow reserve in the ischemic myocardium was found in the rAAV-VEGF-A/PDGF-B group (128 ± 12% vs. 137 ± 10% in nonischemic tissue, p = NS. vs. nonischemic tissue, p < 0.05 vs. the rAAV.Mock group).

Finally, we verified whether the restoration of regional blood flow after transfection with rAAV.VEGF-A/PDGF-B could improve global myocardial function. Although LV end-diastolic pressure did not change significantly over 4 weeks with rAAV.Mock (17.1 ± 1.2 to 19.4 ± 1.0 mm Hg) or rAAV.VEGF-A treatment (15.5 ± 0.6 to 15.8 ± 0.8 mm Hg), combined treatment of rAAV.VEGF-A/PDGF-B reduced LV end-diastolic pressure in the same period from 16.8 ± 0.9 to 12.9 ± 0.9 mm Hg (p = 0.01) (Fig. 5A). Moreover, combined treatment improved ejection fraction from 35.8 ± 2.6% to 55.4 ± 4.1% (p < 0.05), whereas no statistically significant alteration was observed either in the mock- (from 38.1 ± 2.3% to 33.7 ± 2.8%) or the VEGF-A treated group (32.2 ± 1.9% to 37.2 ± 2.1%) (Fig. 5B). Accordingly, the contraction velocity dP/dt$_{max}$ was altered only by VEGF-A/PDGF-B (1,731 ± 104 mm Hg/s vs. 1,337 ± 67 mm Hg/s in rAAV.Mock at rest), but not by VEGF-A therapy (1,275 ± 145 mm Hg/s) (Online Fig. 4A). Relaxation velocity showed the same improvement (dP/dt$_{min}$: −1,854 ± 127 mm Hg/s in the VEGF-A/PDGF-B group vs. −1,206 ± 174 mm Hg/s and −1,080 ±

89 mm Hg/s in the rAAV.Mock and rAAV.VEGF-A groups, respectively) (Online Fig. 4B). To quantify the functional reserve of the ischemic myocardium, analysis of regional shortening of the LV lateral wall by sonomicrometry was performed at rest and at increasing heart rates. As shown in Figure 5C, subendocardial segment shortening in mock-treated hearts was severely impaired at baseline (40 ± 7% of the nonischemic rAAV.Mock level) and steadily declined during pacing, arriving at 9 ± 6% at 150/min (p < 0.05). VEGF-A transduction of the ischemic myocardium did not alter this behavior significantly (42 ± 4% at baseline to 24 ± 4% at 150 beats/min, p < 0.05). In contrast, combined treatment with rAAV.VEGF-A/PDGF-B caused a trend toward functional improvement at rest (64 ± 9%, p = 0.07 vs. rAAV.Mock and rAAV.VEGF-A) and statistically significant benefit at 150 beats/min (53 ± 11%, p < 0.05).

Discussion

In the present pre-clinical study, we used a long-acting vector (AAV) as a means to ensure long-term efficacy of transduction. Moreover, we sought to overcome the weakness of VEGF-A with respect to inducing vessel maturation and collateral growth by combining it with PDGF-B, a factor well-known for its role in mural cell recruitment. In

a peripheral artery occlusion model, we found that the VEGF-A/PDGF-B combination did not alter the capillary density induced by VEGF-A alone (Figs. 1A and 1B). However, pericyte coverage of capillaries as well as growth of the conductance vessels (collaterals) increased significantly after PDGF-B cotransduction (Figs. 1C, 1D, 2A, and 2B), enabling a gain in limb perfusion. Combined VEGF-A/PDGF-B gene therapy was also found capable of improving the function of hibernating myocardium in a large-animal model (pigs) of chronic ischemia, in contrast to VEGF-A alone, even though the latter was given at a 5-fold higher dose (1×10^{13} virus particles vs. 2×10^{12} in the combined group). Again, increased angiogenesis, pericyte coverage, and collateral growth were hallmarks of the combined treatment (Figs. 3 to 5). Earlier gene therapy studies for induction of angiogenesis and/or arteriogenesis frequently used adenoviruses (i.e., vectors capable of intense early efficacy followed by subsequent silencing by the immune system) rendering repeated applications inefficient (25). The intensity of early vector activity may also account for side effects such as irregular capillary network formation (26), potentially harming the residual muscle perfusion and preventing essential collateral growth (13,27). Moreover, adenoviral VEGF-A transduction failed to increase calf capillary density 20 days later, suggesting that vessel regression takes place as a result of short duration of expression (26).

In contrast, if delivered by an AAV, which provides a delayed but prolonged gene expression, VEGF-A was capable of inducing a lasting gain in perfusion (28). However, at the high dose used in that study in the rat hindlimb (1.8×10^{13} virus particles), contamination of noninjected organs such as the brain and testis was found, and muscles secreted VEGF-A readily even after isolation and in vitro cultivation. In our rabbit study using a 360-fold lower virus dose in a >10-fold larger animal, no serum contamination was found (data not shown), whereas reporter gene activity indicated continued muscle cell expression until the end of the observation period. When we applied higher doses (1×10^{13} virus particles), VEGF-A was able to initiate collateralization in the rabbit model (data not shown). In that case, we did not observe hemangioma formation, but found remote target gene expression in the contralateral limb, liver, spleen, and kidney, consistent with a low, but detectable LacZ expression in the rAAV.LacZ group in these organs.

In an attempt to increase safety of a long-acting vector, we used a low dose of 0.5×10^{11} virus particles, at which VEGF-A alone was unable to improve capillary pericyte coverage and collateralization in chronically ischemic hindlimbs (Figs. 1D and 2B). The mechanisms behind this immature vessel growth include high and dishomogeneous VEGF-A levels (inducing irregular capillary networks) (6), as well as a lack of pericyte recruitment (leading to increased vascular permeability). Greenberg et al. (7) recently demonstrated that this effect of VEGF-A is caused by VEGF-R2 mediated inhibition of PDGF-Rβ.

To overcome this lack of efficacy, we added a vector expressing the maturation factor PDGF-B (17,29,30). When applied via retroinfusion, the combination of low-dose VEGF-A (0.5×10^{11} virus particles) and medium-dose PDGF-B (1×10^{12} particles) not only restored capillary maturation by pericyte coverage, without altering the capillary density compared with VEGF-A alone (Figs. 1B to 1D), but also significantly increased collateralization. The result was a profound improvement in perfusion. The effect of PDGF-B on collateral arteries may arise from 2 possible causes: First, the functionally improved microcirculation may activate collateral growth through increased flow and shear stress, a powerful driving force of arteriogenesis (31) that is also observed in the instance of angiopoietin-1 combined with VEGF-A (32,33). Second, a direct effect of PDGF-B on collateral growth cannot be excluded, although this effect appears weaker than that of monocyte chemoattractant protein-1 or basic fibroblast growth factor (30). It should be noted that retroinfusion allows homogeneous transduction of the thigh muscles where local stimulation of collateral growth takes place (34).

Applying the VEGF-A/PDGF-B combination approach to a pig model of hibernating myocardium, we retroinfused a size-adapted VEGF-A dose (2×10^{12} virus particles for a 40-kg animal), with only double the PDGF-B dose (4×10^{12} virus particles) because a high dose of PDGF-B might provoke coronary restenosis formation in the heart (35). The efficacy of the given amount of VEGF-A/PDGF-B was ensured by documentation of increased capillary and collateral counts as well as pericyte coverage (Figs. 3B and 4B). These effects resulted in an increase of myocardial perfusion and function at rest and rapid atrial pacing (Figs. 4D, 4E, and 5A to 5C). In comparison, a 5-fold higher dose of VEGF-A (10^{13} virus particles) could not increase collateralization or perfusion, nor improve cardiac function (Figs. 4 and 5), although angiogenesis was efficiently induced (Fig. 3B). This latter finding suggests that capillary density itself is insufficient to resolve hibernating myocardium.

Conclusions

We studied the efficacy of rAAV-mediated transfer of the genes of VEGF-A and PDGF-B for inducing functionally relevant therapeutic neovascularization after peripheral arterial and coronary artery occlusion. We found that the combination of VEGF-A and PDGF-B exceeded the efficacy of VEGF-A alone, particularly with respect to microvascular maturation and collateral growth, resulting in a significant gain in perfusion and (in the heart model) muscle function. Because the VEGF-A levels chosen were low and no alteration of circulating VEGF levels was found, the combination of VEGF-A and PDGF-B with a long-lasting vector may be therapeutically rewarding in no-option patients with chronic peripheral or cardiac ischemia.

Reprint requests and correspondence: Dr. Christian Kupatt, Medizinische Klinik I Klinikum Großhadern, Ludwig Maximilians University of Munich, Marchioninistrasse 15, 81377 Munich, Germany. E-mail: Christian.Kupatt@med.uni-muenchen.de.

REFERENCES

1. Yla-Herttuala S, Rissanen TT, Vajanto I, Hartikainen J. Vascular endothelial growth factors: biology and current status of clinical applications in cardiovascular medicine. J Am Coll Cardiol 2007;49:1015–26.
2. Rissanen TT, Yla-Herttuala S. Current status of cardiovascular gene therapy. Mol Ther 2007;15:1233–47.
3. Dor Y, Djonov V, Abramovitch R, et al. Conditional switching of VEGF provides new insights into adult neovascularization and proangiogenic therapy. EMBO J 2002;21:1939–47.
4. Jain RK. Molecular regulation of vessel maturation. Nat Med 2003;9:685–93.
5. Grunewald M, Avraham I, Dor Y, et al. VEGF-induced adult neovascularization: recruitment, retention, and role of accessory cells. Cell 2006;124:175–89.
6. von Degenfeld G, Banfi A, Springer ML, et al. Microenvironmental VEGF distribution is critical for stable and functional vessel growth in ischemia. FASEB J 2006;20:2657–9.
7. Greenberg JI, Shields DJ, Barillas SG, et al. A role for VEGF as a negative regulator of pericyte function and vessel maturation. Nature 2008;456:809–13.
8. Ozawa CR, Banfi A, Glazer NL, et al. Microenvironmental VEGF concentration, not total dose, determines a threshold between normal and aberrant angiogenesis. J Clin Invest 2004;113:516–27.
9. Zacchigna S, Tasciotti E, Kusmic C, et al. In vivo imaging shows abnormal function of vascular endothelial growth factor-induced vasculature. Hum Gene Ther 2007;18:515–24.
10. Dor Y, Djonov V, Keshet E. Induction of vascular networks in adult organs: implications to proangiogenic therapy. Ann N Y Acad Sci 2003;995:208–16.
11. Ferrara N. VEGF as a therapeutic target in cancer. Oncology 2005;69 Suppl 3:11–6.
12. Eberhard A, Kahlert S, Goede V, Hemmerlein B, Plate KH, Augustin HG. Heterogeneity of angiogenesis and blood vessel maturation in human tumors: implications for antiangiogenic tumor therapies. Cancer Res 2000;60:1388–93.
13. Hershey JC, Baskin EP, Corcoran HA, et al. Vascular endothelial growth factor stimulates angiogenesis without improving collateral blood flow following hindlimb ischemia in rabbits. Heart Vessels 2003;18:142–9.
14. Deindl E, Buschmann I, Hoefer IE, et al. Role of ischemia and of hypoxia-inducible genes in arteriogenesis after femoral artery occlusion in the rabbit. Circ Res 2001;89:779–86.
15. Deindl E, Schaper W. The art of arteriogenesis. Cell Biochem Biophys 2005;43:1–15.
16. Yla-Herttuala S. An update on angiogenic gene therapy: vascular endothelial growth factor and other directions. Curr Opin Mol Ther 2006;8:295–300.
17. Zymek P, Bujak M, Chatila K, et al. The role of platelet-derived growth factor signaling in healing myocardial infarcts. J Am Coll Cardiol 2006;48:2315–23.
18. Bish LT, Morine K, Sleeper MM, et al. Adeno-associated virus (AAV) serotype 9 provides global cardiac gene transfer superior to AAV1, AAV6, AAV7, and AAV8 in the mouse and rat. Hum Gene Ther 2008;19:1359–68.
19. Lehrke M, Lebherz C, Millington SC, et al. Diet-dependent cardiovascular lipid metabolism controlled by hepatic LXR[alpha]. Cell Metab 2005;1:297–308.
20. Kupatt C, Hinkel R, von Bruhl ML, et al. Endothelial nitric oxide synthase overexpression provides a functionally relevant angiogenic switch in hibernating pig myocardium. J Am Coll Cardiol 2007;49:1575–84.
21. Pinkenburg O, Pfosser A, Hinkel R, et al. AAV-based gene transfer of cathelicidin induces therapeutic neovascularization preferentially via potent collateral growth. Hum Gene Ther 2009;20:159–67.
22. Pfosser A, Thalgott M, Büttner K, et al. Liposomal Hsp90 cDNA induces neovascularization via nitric oxide in chronic ischemia. Cardiovasc Res 2005;65:728–36.
23. von Degenfeld G, Raake P, Kupatt C, et al. Selective pressure-regulated retroinfusion of fibroblast growth factor-2 into the coronary vein enhances regional myocardial blood flow and function in pigs with chronic myocardial ischemia. J Am Coll Cardiol 2003;42:1120–8.
24. Cohen M, Rentrop KP. Limitation of myocardial ischemia by collateral circulation during sudden controlled coronary artery occlusion in human subjects: a prospective study. Circ 1986;74:469–76.
25. Gruchala M, Bhardwaj S, Pajusola K, et al. Gene transfer into rabbit arteries with adeno-associated virus and adenovirus vectors. J Gene Med 2004;6:545–54.
26. Vajanto I, Rissanen TT, Rutanen J, et al. Evaluation of angiogenesis and side effects in ischemic rabbit hindlimbs after intramuscular injection of adenoviral vectors encoding VEGF and LacZ. J Gene Med 2002;4:371–80.
27. Masaki I, Yonemitsu Y, Yamashita A, et al. Angiogenic gene therapy for experimental critical limb ischemia: acceleration of limb loss by overexpression of vascular endothelial growth factor 165 but not of fibroblast growth factor-2. Circ Res 2002;90:966–73.
28. Shimpo M, Ikeda U, Maeda Y, et al. AAV-mediated VEGF gene transfer into skeletal muscle stimulates angiogenesis and improves blood flow in a rat hindlimb ischemia model. Cardiovasc Res 2002;53:993–1001.
29. Lindahl P, Johansson BR, Leveen P, Betsholtz C. Pericyte loss and microaneurysm formation in PDGF-B-deficient mice. Science 1997;277:242–5.
30. Schierling W, Troidl K, Troidl C, Schmitz-Rixen T, Schaper W, Eitenmüller IK. The role of angiogenic growth factors in arteriogenesis. J Vasc Res 2009;46:365–74.
31. Eitenmuller I, Volger O, Kluge A, et al. The range of adaptation by collateral vessels after femoral artery occlusion. Circ Res 2006;99:656–62.
32. Arsic N, Zentilin L, Zacchigna S, et al. Induction of functional neovascularization by combined VEGF and angiopoietin-1 gene transfer using AAV vectors. Mol Ther 2003;7:450–9.
33. Pajusola K, Kunnapuu J, Vuorikoski S, et al. Stabilized HIF-1alpha is superior to VEGF for angiogenesis in skeletal muscle via adeno-associated virus gene transfer. FASEB J 2005;19:1359–68.
34. Lebherz C, von Degenfeld G, Karl A, et al. Therapeutic angiogenesis/arteriogenesis in the chronic ischemic rabbit hindlimb: effect of venous basic fibroblast growth factor retroinfusion. Endothelium 2003;10:257–65.
35. Levitzki A. PDGF receptor kinase inhibitors for the treatment of restenosis. Cardiovasc Res 2005;65:581–6.

Key Words: angiogenesis ■ arteriogenesis ■ gene therapy ■ pericytes.

▶ **APPENDIX**

For additional figures, please see the online version of this article.